ELSEVIER

Journal of Neuroimmunology 137 (2003) 67–78

Journal of Neuroimmunology

www.elsevier.com/locate/jneuroim

Characterization of the acute immune response in the retina of Borna disease virus infected Lewis rats

Tobias Stahl[a,*], Christopher Mohr[a], Johannes Kacza[a], Christine Reimers[a], Thomas Pannicke[b], Christian Sauder[c], Andreas Reichenbach[b], Johannes Seeger[a]

[a] *Department of Veterinary Anatomy, University of Leipzig, An den Tierkliniken 43 D-04109 Leipzig, Germany*
[b] *Department of Neurophysiology, Paul Flechsig Institute for Brain Research, University of Leipzig, Leipzig, Germany*
[c] *Department of Virology, Institute for Medical Microbiology and Hygiene, University of Freiburg, Freiburg, Germany*

Received 4 September 2002; accepted 27 January 2003

Abstract

In Lewis rats infected intracerebrally with the highly neurotropic Borna disease virus (BDV), the retina is one of the most severely affected central nervous system (CNS) structures. While BDV-induced damage in the brain has been previously shown to be caused by a T-cell-dependent process, the immunopathological mechanisms leading to BDV-induced retinitis remain to be elucidated.

RNA samples from retinae were subjected to RNase protection assays to detect transcripts of proinflammatory cytokines and chemokines known to be involved in the recruitment of T-cells and macrophages in the CNS.

The observed expression profile of proinflammatory cytokines and chemokines, as well as the immunohistochemical detection of αβTCR-positive, CD4- and CD8-positive T-cells in the BDV-infected retinae, is reminiscent of the situation observed in the brains of Lewis rats during the acute phase of Borna disease (BD). This suggests that similar immunopathological mechanisms are operating in retinae and brains of infected rats.

Keywords: Retina; Borna disease virus; CD4; CD8; Proinflammatory cytokines; Chemokines; Lewis rat

1. Introduction

Borna disease virus (BDV) is the causative agent of Borna disease (BD), an inflammatory central nervous system (CNS) disease naturally occurring in horses and sheep, but also in a variety of other species (for review see Staeheli et al., 2000). Based on its unique genetic and biologic properties, BDV is considered to be the prototypic member of a new virus family, *Bornaviridae*, within the order *Mononegavirales* (de la Torre, 1994; Schneemann et al., 1995).

During recent years, BDV-infection of rats has been proven to represent a valuable model to study a neurological disease that is characterized by behavioural and motility disturbances and blindness (Narayan et al., 1983a,b; Stitz et al., 1995). In the brain these neurological defects could be attributed to a CD4+ T-cell dependent immunopathological mechanism where CD8+ T-cell mediated processes are operative (Richt et al., 1989; Planz et al., 1993, 1995; Stitz et al., 1995; Noske et al., 1998). An elevated expression of several proinflammatory cytokines, and of chemokines with T-cell and monocyte chemoattractant characteristics, has been described in brains of infected rats (Shankar et al., 1992; Morimoto et al., 1996; Hatalski et al., 1998; Sauder and de la Torre, 1999; Sauder et al., 2000). These soluble mediators play crucial roles in the shaping of the inflammatory cascade resulting in a recruitment of lymphocytes and monocytes into the CNS. After intracerebral BDV-inoculation in adult Lewis rats, the virus spreads in all brain regions where it predominantly infects neurons, but also astrocytes (Carbone et al., 1991, 1993). The infection leads to a disseminated nonpurulent meningoencephalitis. In surviving animals, the virus persists in the CNS. Highest virus titers have been found in the cerebrum and the retina (Narayan et al., 1983a). The pathomorpho-

* Corresponding author. Tel.: +49-341-9738034; fax: +49-341-9738029.
E-mail address: stat@medizin.uni-leipzig.de (T. Stahl).

0165-5728/03/$ - see front matter © 2003 Elsevier Science B.V. All rights reserved.
doi:10.1016/S0165-5728(03)00044-4

logical characteristics of the BDV-infected brain are degenerating neurons, predominantly in the hippocampal formation and the frontoparietal cortex (Deschl et al., 1990; Narayan et al., 1983a). In addition, massive astrocytosis and microglial activation take place in the infected brain (Deschl et al., 1990; Gonzalez-Dunia et al., 1997). Immune cell infiltrates in the rat brain mainly consist of CD4+, CD8+ cells and macrophages (Deschl et al., 1990; Hatalski et al., 1998).

Neurodegenerative processes in the visual system, resulting in blindness, have been reported in BDV-infected rats, rabbits, rhesus monkeys (*Macaca mulatta*) and horses (Krey et al., 1979a; Stitz et al., 1981; Narayan et al., 1983a; Bilzer et al., 1995; Kacza et al., 2000). In contrast to the brain, only very limited, notably morphological data, exist on the composition of immune cell infiltrates as well as on the spectrum of soluble immunomodulatory factors in the retina. In the BDV-infected rat, synchronous infection of both retinae occurs within 15–20 days after intracerebral inoculation, and leads to a massive degeneration of retinal neurons (Narayan et al., 1983a; Kacza et al., 2000). Microglia and macrophages have been identified as main components of retinal infiltrates (Geiss et al., 1990; Kacza et al., 2000), whereas only a few lymphocytes, which were designated to be plasma cells, were detected (Geiss et al., 1990). The main glial element of the retina, the Müller cells, show slightly enhanced GFAP-expression and faint electrophysiological alterations (Pannicke et al., 2001; Kacza et al., 2001).

The aim of the work described here was to identify cellular elements and soluble factors involved in BDV-induced inflammation in the retina, a CNS region constantly and heavily affected in rats infected with BDV.

Immunohistochemically, we provide first evidence that T-cells represent a component of early retinal infiltrates. Furthermore, data are presented that elucidate the expression profile of proinflammatory cytokines and T-cell-acting chemokines in the BDV-infected retina.

2. Materials and methods

2.1. Animals

The animal experiments were approved by the Independent Ethical Committee of the Regierungspräsidium Leipzig, License No. TVV 3/2001. Lewis rats (LEW/CRL BR) were purchased from Charles River (Sulzfeld, Germany) and bred in the experimental center of the Medical Faculty, University of Leipzig. Infections of animals were done under anesthesia (ketamine/xylazine).

2.2. Infection of rats

The BDV stock used in the experiments was the first passage of the Giessen strain He/80 (kindly provided by J. Richt, Giessen) in adult Lewis rats. Stock homogenates were prepared 4 weeks pi and stored at −70 °C till used for infection. Four-week-old Lewis rats were inoculated intracranially by injection into the left brain hemisphere with 50 μl BDV stock homogenate diluted in RPMI-1640. As control, animals were mock infected with a rat brain homogenate diluted in the same medium.

2.3. Preparation of retinae for histological and immunohistochemical analysis

Immediately after the death of the animals, they were perfused transcardially with 0.1 M phosphate buffered saline (PBS) followed by perfusion with 4% paraformaldehyde (PFA) in the same buffer. For detection of CD4-positive cells, of glial fibrillary acidic protein (GFAP) positive cells and of microglial cells, perfusion with fixative was omitted.

Dissected retinae of animals perfused with PFA were postfixed in the same fixative, and cryoprotected in 30% sucrose overnight. Fixed and unfixed retinae were embedded in Tissue-Tek OCT compound (Sakura) and snap frozen at −40 °C. Ten-micrometer-thick sections were cut with a cryostat (Microm, Walldorf, Germany), mounted onto poly-L-lysine coated slides and stored at −20 °C until being used. Unfixed retina slices were fixed in 4% PFA or in isopropyl for 5 min at room temperature prior to the staining procedure.

2.4. Preparation of RNA

To minimize contamination of retinal tissue with intravasal cells, rats were perfused with PBS. Subsequently, eyes were enucleated, retinae dissected and stored in RNA-later (Ambion, TX, USA) at −20 °C till RNA-extraction. Total RNA from dissected retinae was isolated using the RNAclean™ method (AGS, Hybaid, Heidelberg, Germany) according to manufacturer's specifications. Precipitated RNA samples were dissolved in 0.5 mM EDTA and stored at −70 °C. Quality and quantity of total RNA prepared was evaluated photometrically and by electrophoresis.

2.5. Immunohistochemical and histological analysis

For histological analysis, retinae were stained either with hematoxylin/eosin or methylene blue.

Except for the visualization with diaminobenzidine (DAB), all steps of the immunohistochemical procedure were performed in 0.1 M Tris-buffered saline pH 7.4 (TBS). Endogenous peroxidase activities were abolished by incubation of the specimens with 0.3% hydrogen peroxide in TBS for 15 min. Unspecific binding sites were quenched by incubation of slides in TBS containing 5% normal goat serum (blocking solution) just prior to the incubation of slides with primary antibodies in blocking solution at 4 °C overnight. For detection of pan T-cells, a monoclonal antibody (mAb) against rat αβ T-cell receptor

(αβTCR) (clone R73; gift of J. Richt, Giessen; dilution 1:10), for detection of CD4-positive cells the mAb W3/25 (Serotec, Oxford, UK; dilution 1:500) and for detection of cytotoxic T-cells and NK cells an mAb against CD8 (Ox8, Serotec; dilution 1:200) was used. The CD45R antibody (clone HIS24, pan B-cell, Pharmingen; 1:200) was used for the detection of B-lymphocytes. Specimens from lymph nodes processed in parallel served as positive control. For virus antigen detection, an mAb recognizing the BDV-nucleoprotein p40 (Bo 18; gift of J. Richt, Giessen; dilution 1:100) was used. Retinal Müller cells were detected with a polyclonal rabbit serum against GFAP (DAKO, Denmark) at a 1:2000 dilution. For recognition of microglia/macrophages, the Ox42 antibody, specific for rat CD11b, (Serotec; dilution 1:200) was used. Control experiments were done either by omitting incubation with the primary antibody or by using mouse IgG2b (Serotec; dilution 1:100) as a primary antibody. Incubation with primary antibodies was followed by incubation with a rat adsorbed, biotin conjugated goat-anti-mouse IgG (1:400, Dianova, Hamburg, Germany) or with a biotinylated goat-anti-rabbit IgG (DAKO; 1:1000), respectively. Bound secondary antibodies were revealed with an avidin–biotin–peroxidase kit (ABC, Vector Laboratories) and DAB as a substrate.

2.6. Ribonuclease protection assay

A commercially available multiprobe template set allowing generation of riboprobes to detect transcripts of interleukin (IL) 1α, IL1β, IL2, IL3, IL4, IL5, IL6, IL10, tumor necrosis factor (TNF) α, TNFβ and interferon (IFN) γ was used for the investigation of rat cytokines (rCK-1, Pharmingen, San Diego, CA, USA). Plasmids used for rat chemokine riboprobe synthesis are described in detail elsewhere (Sauder et al., 2000). Partial sequences of rat XCL1 (lymphotactin), CCL2 (monocyte chemotactic protein-1, MCP-1), CCL4 (macrophage inflammatory protein-1β; MIP-1β), CCL5 (RANTES), CXCL10 (interferon inducible protein-10; IP-10) and mouse L32, subcloned into pGEM-3Z vector, were linearized using the restriction enzyme *Hind*III. Following purification, the linearized plasmids were pooled as a template set with a final concentration of 50 ng/μl each. The ribosomal protein L32 (encoded by a housekeeping gene) included in both the chemokine and cytokine template set was used for normalization of expression of monitored genes. In vitro transcription of riboprobes, hybridization and RNase treatments were done according to the manufacturer's instructions (RiboQuant™, Pharmingen). For radiolabeling, 100 μCi [α-^{32}]P-UTP (3000 Ci/mmol) was used in a final volume of 20 μl. After riboprobe transcription, templates were digested with DNase I. Labeled probes were extracted with phenol–chloroform, precipitated in ethanol, dried and dissolved in hybridization buffer. Retinal target RNA (10 μg) was vacuum dried and resuspended in 8 μl hybridization buffer. For hybridization, radiolabeled probe set was added at a final concentration of 4×10^5 cpm/μl for the chemokine set and of 8×10^5 cpm/μl for the cytokine set. Samples were denatured at 90 °C for 1–2 min, slowly cooled to 56 °C and incubated at 56 °C in a thermocycler for 14 to 16 h. After RNase and Proteinase K treatment, the protected RNA was phenol–chloroform extracted, precipitated, washed with ethanol, dried and resuspended in the gel loading buffer supplied by the manufacturer. RNA was separated electrophoretically on polyacrylamide gels containing 8 M urea. Dried gels were exposed to phosphoimager plates (Kodak). For quantitative analysis scanned images were analyzed with the multianalyst software (Kodak, Germany).

For statistical analysis, mean values of RNA expression levels of mock-infected and BDV-infected animals were compared by a two-tailed Student's *t*-test.

3. Results

3.1. Clinical observations

All BDV-infected rats developed signs of a severe neurological disorder by day 30 after infection, with hunched body posture, paresis of the hind limbs and rough fur. Weight and size of the infected animals was reduced as compared to mock-infected littermates.

Indirect ophthalmoscopic examination at survival times ranging from 2 weeks to almost 6 months showed no obvious signs of inflammation in the fundus of the infected animals.

3.2. Detection of virus antigen in the retinae of infected rats

To assess the spatial and temporal distribution of BDV-antigen in the retinae of infected rats, we performed immunohistochemical staining using a mAb specifically recognizing the BDV-nucleoprotein p40 that is abundantly expressed in infected tissues (Stitz et al., 1998) (Fig. 1).

Whereas no expression of p40 protein was detectable at 14 days pi (Fig. 1A), the protein could be demonstrated in all retinae studied at 21 days pi in the nerve fiber layer (NFL), the ganglion cell layer (GCL) and the inner plexiform layer (IPL) (Fig. 1B). At day 25 pi, p40-specific staining was additionally found in neuronal somata of the inner nuclear layer (INL) and in the outer plexiform layer (OPL) (Fig. 1C,F). Thirty-one days pi, all retinae investigated displayed nucleoprotein immunoreactivity in all retinal layers, except for the photoreceptor layer (PRL), where specific staining was virtually absent (Fig. 1D,G). No expression of the nucleoprotein was detected in the nonneuronal retinal pigment epithelium (RPE) and in the lamina choriocapillaris.

3.3. Detection of lymphocytes in the infected retinae

Histological examination revealed mononuclear cells infiltrating the retina particularly in the PRL and in close

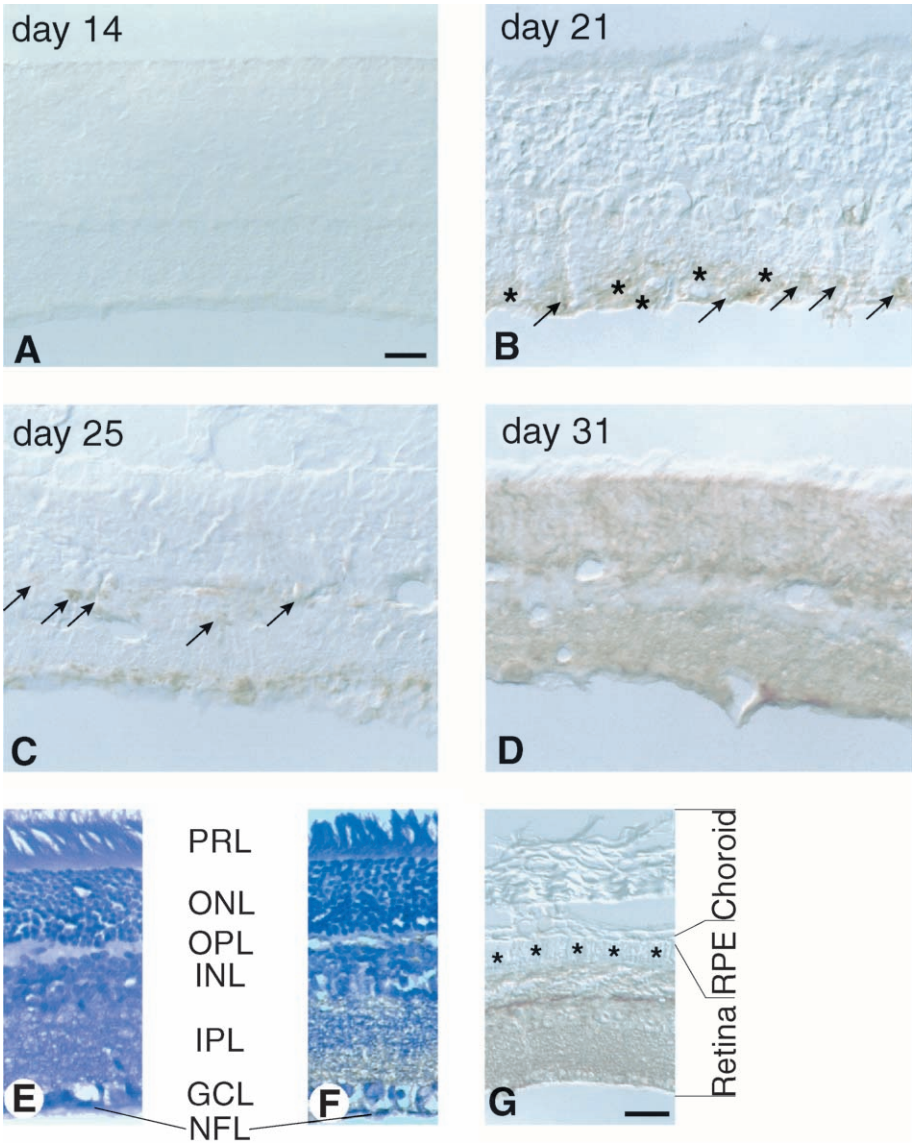

Fig. 1. Immunohistochemical analysis of the distribution of BDV-nucleoprotein (p40) with mAb Bo18 in retinae of mock-infected (E) and BDV-infected rats (A–D, F, G) at different time points post infection (pi). Whereas by day 14 pi no p40 protein was detectable (A), 21 days pi neuronal somata in the ganglion cell layer (GCL) (B, arrows), the nerve fiber layer (NFL) and the inner plexiform layer (IPL) were labeled (B, asterisks). At 25 days pi p40-immunoreactivity was additionally found to be present in the inner nuclear layer (INL) (C, arrows). Thirty-one days post BDV-infection p40 expression was detected in the outer plexiform layer (OPL) and the outer nuclear layer (ONL) (D, G). No p40-specific staining was found in the photoreceptor layer (PRL) (G, asterisks), the retinal pigment epithelium (RPE) and the choroid (G). Photomicrographs E and F display cryostat sections of retinae processed on the day 25 post mock- (E) and BDV-infection (F) counterstained with methylene blue. The scale bar depicted in panel A applies to A–F and represents 20 μm. The scale bar in G represents 40 μm.

proximity to vessels in the inner plexiform layer (IPL) by day 25 pi (not shown). To reveal the involvement of lymphocytes in these infiltrates, immunohistochemical examination was performed with monoclonal antibodies against αβTCR, CD4, CD8 and CD45R. Staining of lymph nodes, processed in parallel with the examined retinae, served as a positive control and revealed the tissue-specific pattern of lymphocyte distribution. Accordingly, both B-cells localized to follicles in the cortical zone, and T-cells were present predominantly in paracortical areas (data not shown).

Retinae were examined 14, 21, 25 and 31 days pi. No lymphocytes were found in the histologically inconspicuous retinae at 14 days post BDV-infection (not shown). Only single T-cells were found in central retinal areas in three out of eight retinae investigated 21 days pi (Fig. 3A).

Employing three different T-cell specific antibodies, several T-cells/NK-cells were detected in infected rats at days 25 and 31 pi in the inner layers (NFL, GCL, IPL) in close vicinity to intraretinal vessels (Fig. 2A,B). Twenty-five days pi scattered parenchymal infiltrates of T-cells were found in all retinae investigated. Larger infiltrates, extending

over all retinal layers, were only found in 5 out of 19 retinae investigated 25 and 31 days pi (Fig. 2E,F). No T-cells were detected within the retinae of mock-infected control animals at any time point investigated (Fig. 3D). Whereas very few T-cells (one to three T-cells per five retinal slices investigated) were detected in the underlying choroidal tissue of the control animals, the frequency of these choroidal T-cells was increased in the infected animals (Fig. 2C,D). Choroidal T-cells were often observed in close relation to the blood vessels (Fig. 2C,D). Besides an increased number of T-cells in the outer retinal layers 31 days pi there were no obvious differences in number and distribution of CD4-positive, CD8-positive or R73-positive T-cells between days 25 and 31 pi (Fig. 2A,B; Fig 3B,C). The distribution of CD4-

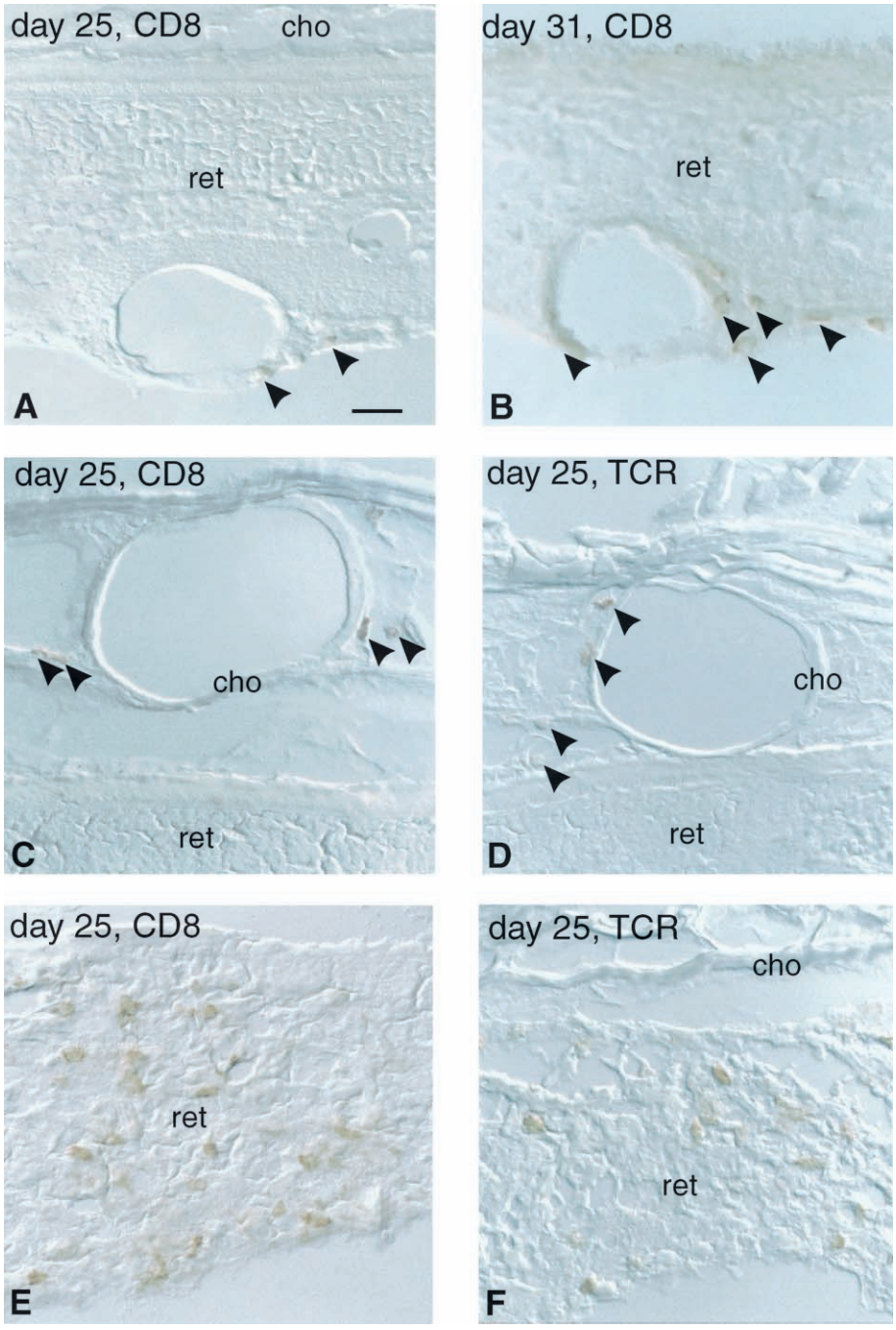

Fig. 2. Immunohistochemical detection of T-lymphocytes with antibodies against the αβ T-cell receptor (TCR) and CD8 in cryostat sections 25 and 31 days pi. At both time points, the immunoreactive cells were typically localized within the inner retinal layers in close vicinity to intraretinal vessels (A, B; arrowheads). Bulbi of BDV-infected animals displayed an increased number of choroidal T-cells located attached to and around large blood vessels (C, D; arrowheads). Photomicrographs E and F are consecutive sections of a large retinal infiltrate, where αβTCR-immunoreactive and CD8-immunoreactive T-cells were found to be present in all retinal layers. The scale bar in panel A applies to all images and represents 20 μm; cho—choroid, ret—retina.

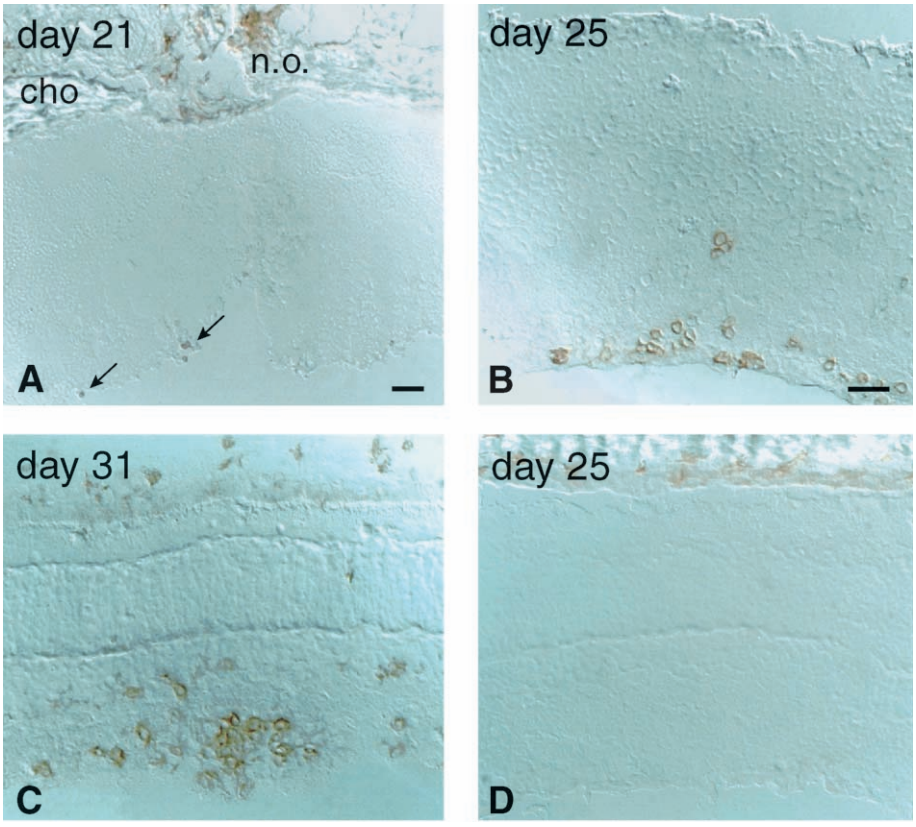

Fig. 3. Detection of CD4-T-cells with the mAb W3/25 in retinal cryostat sections of BDV-infected (A–C) and mock-infected rats (D). At 21 days pi single CD4-T-cells were found in the GCL in central retinal areas (A, arrows). Much larger numbers of CD4-positive cells were found 25 and 31 days pi (B, C). No CD4-positive cells were found in the retinae of mock-infected animals (D). The scale bar in panel A represents 50 μm. The scale bar in panel B applies to photomicrographs B, C and D and represents 20 μm; cho—choroid, n.o.—optical nerve.

positive cells correlated with the distribution of R73-positive T-cells in consecutive sections (not shown).

At day 25 pi, CD45R-positive cells, indicative of B-cells, were predominantly found in the innermost retinal layers similar to the localization of T-cells (Fig. 4A,B). In addition to T-cells, an enhanced number of B-cells localized to the choroid was observed (Fig. 4C). CD45R-positive cells were found only rarely in rat bulbi 31 days pi.

3.4. Activation of retinal glial cells in infected rats

The involvement of retinal glial cells in the early phase of the BDV-induced retinitis was analyzed by immunohistochemistry using a GFAP-specific antibody recognizing astrocytes and an antibody against CD11b (Ox42) as a marker for microglia/macrophages, respectively. Staining of retinal Müller cells with the GFAP antiserum revealed

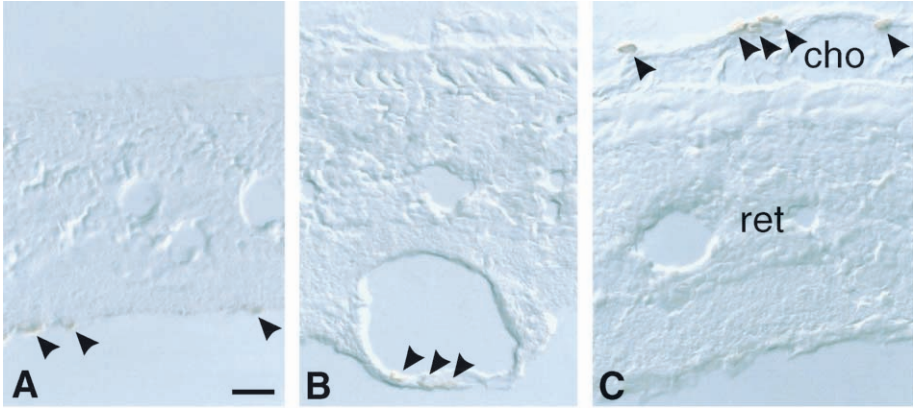

Fig. 4. Detection of B-lymphocytes with the CD45R specific antibody in cryostat sections of rat bulbi 25 days post BDV-infection. B-lymphocytes were typically found to be located in the inner retinal layers (A) and in contact to intraretinal vessels (B). In the choroid (cho), an increased number of CD45R immunoreactive cells were detected (C). The scale bar in panel A, applying to all images, represents 20 μm; ret—retina.

an up-regulation of GFAP in these cells 25 days post BDV-infection (Fig. 5A,B). At the same time Ox42-immunostaining indicated a strong up-regulation of CD11b in the inner retinal layers and the appearance of macrophages in the outer part of the BDV-infected retina (Fig. 5D). In retinae of mock-infected animals, only a weak Ox42-staining of single microglial cells was observed. Macrophages were not detected (Fig. 5C).

3.5. Cytokine expression

A commercially available multiprobe set was used to monitor by ribonuclease protection assay (RPA) the expression profile of proinflammatory (IL1α, IL1β, IL2, IL3, IL5, IL6, TNFα, TNFβ) and anti-inflammatory cytokines (IL4, IL10) during the first 36 days after intracerebral BDV-infection. The expression of the ribosomal protein L32 was measured for normalization of samples. Total RNA was prepared from retinae following perfusion of the rats. At day 21 pi, expression of cytokine transcripts was found to be unchanged in all retinae investigated except for one retina that exhibited slightly elevated expression of mRNA coding for IL1α, IL1β, IL6, IL10, TNFα, TNFβ and IFNγ (Fig. 6A). Enhanced expression of these transcripts was also observed 25, 31 and 36 days after BDV-infection, with the exception of the IL6 mRNA, which was only elevated in retinae of BDV-infected rats, sacrificed 25 and 31 days pi (Fig. 6B,C). No constitutive cytokine mRNA-expression was found in mock-infected animals at the stages investigated here.

At all times investigated, mRNA expression levels of proinflammatory cytokines IL1β and TNFα appeared to be more abundant, compared to the expression of the other cytokine transcripts found to be elevated in the BDV-infected retina (Fig. 6A–D).

3.6. Chemokine expression

We have shown that retinal infiltrates are characterized by both T-cells and macrophages. To answer the question whether T-cell and macrophage attracting chemokines are

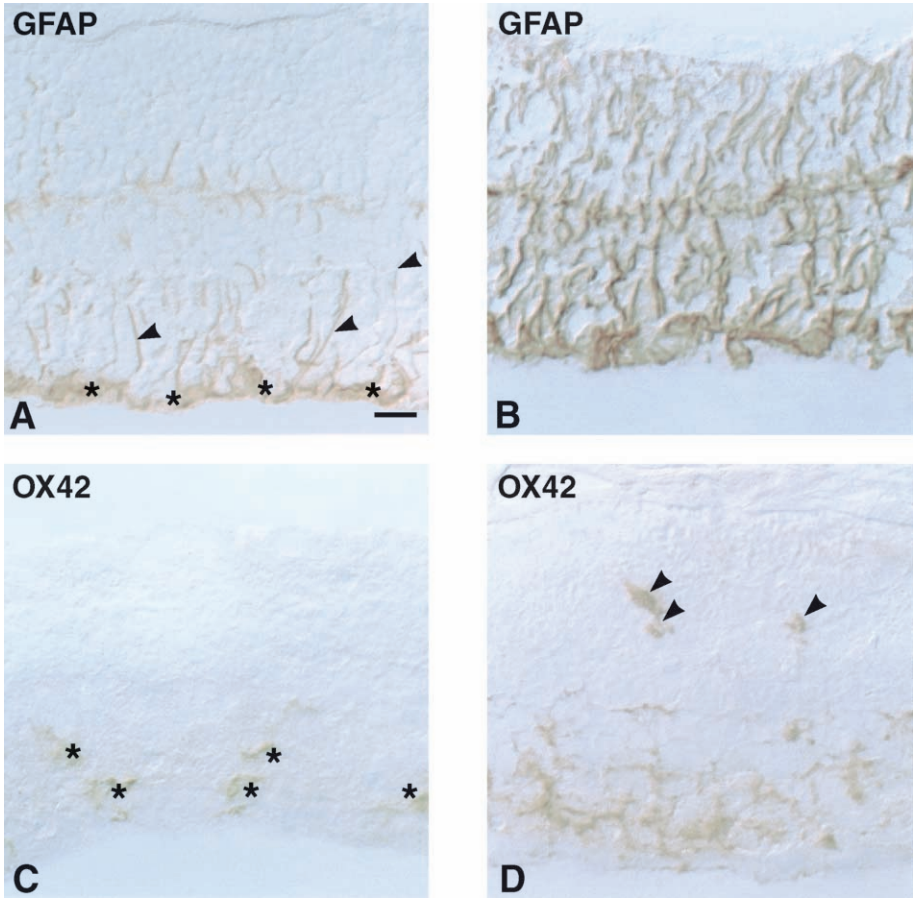

Fig. 5. Labeling of retinal Müller cells and astrocytes with a GFAP antiserum and of microglial cells with the Ox42 antibody in retinae obtained from mock- (A, C) and BDV- (B, D) infected animals 25 days post infection. In retinae of mock-infected animals, the GFAP antiserum only labels Müller cell endfeet and astrocytes in the NFL (A; asterisks) and Müller cell processes predominantly in the IPL (A; arrowheads). After BDV-infection, Müller cells display an enhanced GFAP-expression throughout all retinal layers (B). In control animals, only a few single microglial cells, located in the NFL, GCL and IPL, express Ox42 (C; asterisks). A dense network of microglial cells was labeled in the BDV-infected retina (D). In the outer retinal layers, several more round shaped, Ox42-immunoreactive macrophages were observed (D, arrowheads). The scale bar in panel A, applying to all images, represents 20 μm.

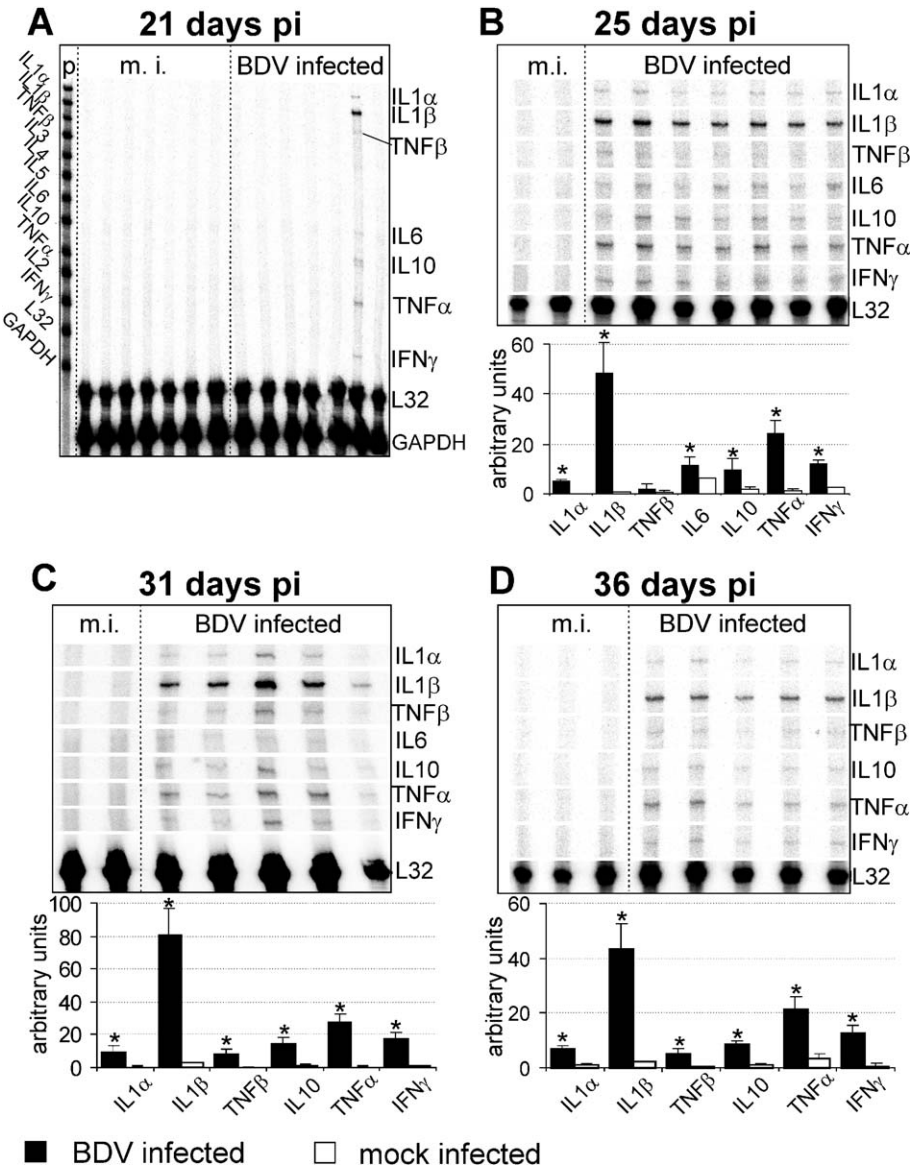

Fig. 6. Kinetics of expression of various cytokine genes in retinae of BDV-infected Lewis rats analyzed by RPA. Total RNA samples (10 μg) from whole retinae of mock-infected (m.i.) and BDV-infected rats sacrificed at 21, 25, 31 and 36 days pi were subjected to RPA. Notations on the left of the first autoradiograph indicate positions of the undigested probes (A; p). The identities of the protected probes hybridized with cytokine transcripts obtained from BDV-infected or mock-infected (m.i.) retinae each are indicated on the right (A–D). Expression of L32 transcripts was used for normalization of expression of monitored cytokine genes. Densitometric quantification of the cytokine gene expression at 25, 31 and 36 days pi is given below the autoradiographs. Black columns represent mean values (± S.E.M.) from BDV-infected animals, white columns represent mean values (± S.E.M.) from mock-infected animals. *Differences are statistically significant at $P < 0.05$.

expressed in infected retinae, RPA for a number of chemokines were performed. Chemokines are low molecular weight chemotactic cytokines. Based on the position and the number of their first conserved cysteine residues they are classified into four groups, CXC, CX_3C, CC and C (Zlotnik and Yoshie, 2000). Most CC chemokines, such as CCL2, CCL4 and CCL5 are chemoattractants for monocytes. CCL2 and CCL5 also attract T-cells. The CXC-chemokine CXCL10 is particularly involved in the recruitment of activated T-cells and NK-cells. The only known member of the C-chemokine family in rodents, XCL1, seems to play a role in attraction of both T-cells and macrophages (for review see Hesselgesser and Horuk, 1999).

To study chemokine gene expression in retinae of BDV-infected rats, we used an RPA multiprobe set that allows the analysis of transcripts of rat chemokine genes coding for XCL1, CCL2, CCL4, CCL5 and CXCL10. Retinae were investigated 25 days pi, i.e., when lymphocytes were first found to infiltrate the BDV-infected retinae, and 36 days pi. None of the chemokines investigated was found to be expressed in control retinae. Twenty-five days after infection, expression of all chemokine transcripts investigated

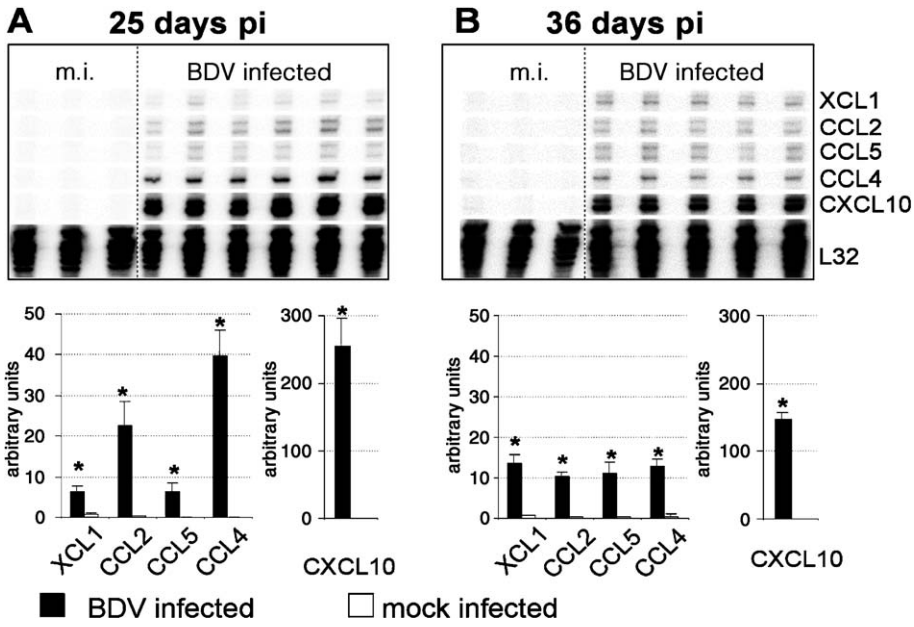

Fig. 7. Kinetics of expression of various chemokine genes in retinae of BDV-infected Lewis rats analyzed by RPA. Autoradiographs depicted display RPA-analysis of total RNA, isolated 25 and 36 days post mock-infection (m.i.) or BDV-infection. Denomination of the protected probes is given in B. Columns indicate mean values (± S.E.M.) of relative RNA-content calculated by normalizing the band intensities against the corresponding L32 transcript levels. See Section 2.6 for further information. *Differences are statistically significant at $P < 0.001$.

was markedly increased with expression being most prominent for CXCL10, CCL2 and CCL4 (Fig. 7A). In retinae investigated at day 36 pi, expression of the latter two chemokines was reduced to levels comparable to XCL1 and CCL5 (Fig. 7B). CXCL10-expression also decreased at this time point but was still remarkably higher than expression of the other chemokines investigated (Fig. 7B).

4. Discussion

Our previous studies, analyzing the BDV-induced retinitis at 5 weeks to 8 months pi, revealed a strong activation of resident microglia and macrophages accompanied by a massive degeneration of all retinal neurons (Kacza et al., 2000, 2001).

The present study was performed to address the question whether this picture represents a region-specific primary reaction, where T-cell independent mechanisms might be active, or alternatively, the result of a pathogenic process comparable to that observed in the brains of BDV-infected Lewis rats.

In all retinae of animals sacrificed 21 days or later following intracranial BDV-infection, the viral nucleoprotein was detected by immunocytochemistry. Nucleoprotein immunoreactivity was first found in the NFL and the GCL, indicating the optic nerve as the entrance route of infectious BDV. This observation is consistent with earlier findings in rabbits, where dissection of the optic nerve prevented retinal infection and subsequent retinopathy (Krey et al., 1979b). The failure to detect the nucleoprotein in adjacent choroid tissue, and the observed stepwise spread of nucleoprotein expression towards the outer retinal layers further support the transneuronal trafficking of infectious virus towards and inside the retina.

The neurodegenerative effects in the brain of BDV-infected rats have been shown to be the result of a T-cell-mediated delayed-type hypersensitivity reaction in which CD8 T-cells are the main effector cells triggering the immune response (Stitz et al., 1995). Here we show, for the first time, the entry of CD8 and αβTCR expressing lymphocytes into the BDV-infected retina. The typical localization of these T-cells within the vascularized inner retinal layers permits the assumption that these T-cells enter the retina via the endothel of intraretinal blood vessels. Activated T-cells are able to bind to RPE cells (Mesri et al., 1994) and transmigrate through the RPE-mediated blood–retina barrier following activation of the RPE cells by IFNγ (Devine et al., 1996). The observed accumulation of choroidal T-cells and of a few T-cells located in the PRL indicate that the Bruch's membrane and the RPE cells may constitute a second entrance route of lymphocytes during retinal BDV-infection.

Consistent with earlier observations in the brains of BDV-infected rats (Deschl et al., 1990; Hatalski et al., 1998), B-cells were detected in the BDV-infected retina 25 days pi. In contrast to these studies, describing an increase in the number of B-cells/plasma cells during the acute stage of BD, in the retina only rare B-cells were detected 31 days pi. Notably, the antibody used in our

experiments does recognize the B-cell form of leucocyte common antigen, therefore labeling premature B-lymphocytes but no mature B-cells and plasma cells (Kroese et al., 1987). For this reason, the presence of the latter at 31 days pi cannot be excluded.

Invasion of T-cells into the brain is absent or significantly reduced in immunosuppressed BDV-infected rats (Narayan et al., 1983a,b) as well as in neonatally infected rats, which develop immunotolerance (Herzog et al., 1984). Whereas several factors such as the proinflammatory cytokines TNFα, IL1α/β and IL6, and the chemokines CXCL10, CCL5 and CCL4 are still expressed in the brains of these animals (Morimoto et al., 1996; Sauder and de la Torre, 1999; Hornig et al., 1999; Sauder et al., 2000), the lymphokine IFN-γ is exclusively expressed in the brains of immunocompetent animals which develop a strong T-cell response (Morimoto et al., 1996).

In addition to the proinflammatory cytokines IL1α/β, IL6, TNFα and β, also IFNγ was expressed as early as at day 21 post BDV-infection in one out of seven retinae investigated. It is conceivable that IFNγ, most likely secreted by intraretinal or intrachoroidal T-cells/NK cells, triggers changes at the blood–retina barrier that subsequently facilitate additional accumulation of T-cells in the retina. At day 25 pi, expression of the proinflammatory cytokines IL1α/β, IL6, TNFα and β, IFNγ was up-regulated in all retinae investigated. At this time point, several T-cells and macrophages were found in the retinae of infected animals suggesting that these infiltrating cells contribute to the observed cytokine expression within in the CNS (Zhao and Schwartz, 1998; Munoz-Fernandez and Fresno, 1998).

Results obtained from several brain regions of neonatally BDV-infected rats, suggest that the increased expression of cytokines IL1α/β, IL6 and TNFα in these regions is mediated by reactive astrocytes and microglia (Sauder and de la Torre, 1999). After induction of experimental autoimmune uveitis (EAU), retinal astroglia and microglia release proinflammatory cytokines IL1β and TNFα (Gullapalli et al., 2000). In the BDV-infected retina, Müller cells as well as microglia are activated as evidenced by up-regulated GFAP and Ox42 immunoreactivity, respectively. RPE cells, specialized glial cells, presumably present in the retinal tissue preparations used for RNA-extraction, are capable of cytokine expression. TNFα is constitutively released by RPE cells in the rat retina (de Kozak et al., 1994). Among certain other cytokines, IL1 and IL6 were found to be released by RPE cells upon stimulation with IL1 and TNFα (reviewed in Holtkamp et al., 2001).

The second clinical stage of BDV-infected animals is characterized by an increase of cytokines such as IL4 and TGFβ, involved in the down-regulation of the cellular immune response. In the brain, both Th2-cytokines were slightly enhanced already during the acute phase of BD (Hatalski et al., 1998). In contrast to IL4-expression, IL10-expression was slightly enhanced 21, 25, 31 and 36 days post BDV-infection. IL10 belongs to the group of cytokines typically expressed by CD4 + Th2 cells. However, resident cells, in particular, retinal microglia (Broderick et al., 2000) cannot be excluded as potential source of IL10-mRNA.

Finally, we investigated the expression of chemokines primarily acting on T-cells and macrophages. We found a high conformity of the chemokine pattern in the retina with that previously described in the brain of BDV-infected rats (Sauder et al., 2000). As in the brain the CXCL10 gene was expressed more prominently than other chemokine genes in the BDV-infected retina. Prominent expression of CXCL10 has also been observed in brains of mice infected with lymphocytic choriomeningitis virus, mouse adenovirus type 1 or mouse hepatitis virus (Asensio and Campbell, 1997; Charles et al., 1999; Lane et al., 1998). Thus, the chemokine gene expression pattern in the BDV-infected retina displays similarities to a chemokine expression profile frequently observed in virus-induced CNS inflammation.

With the exception of XCL1, expression of all chemokines investigated can be attributed to astrocytes and microglia activated in response to viral infections (for review see Glabinski and Ransohoff, 1999).

While CXCL10 has previously been found to be present in the aqueous humor of patients suffering from acute anterior uveitis (Verma et al., 1997) or from diabetic retinopathy (Elner et al., 1998), in this study CXCL10-expression could for the first time be directly localized to the retina. Sauder et al. (2000) provided evidence, supporting the conclusion that astrocytes represent the major source of CXCL10 gene expression in the BDV-infected rat brain. A particular prominent expression of CXCL10 was found in the cerebellar Bergmann glia. These astrocytes share a variety of similarities with retinal Müller cells, suggesting the latter, in addition to retinal astrocytes, as a possible source of the retinal CXCL10-expression observed in our study.

CCL2 and CCL4, two other chemokines found to be markedly elevated in the BDV-infected retina, were shown to be expressed by human RPE cells and by retinal endothelial cells upon stimulation with IL1β and TNFα (Crane et al., 2000). Furthermore, in the rabbit retina, IL1β was shown to be capable of inducing the expression of CCL2 by perivascular macrophages and astrocytes (Cuff et al., 2000).

Since we observed an elevated expression of IL1β and TNFα in infected retinae, it is likely that these molecules contribute to the triggering of retinal chemokine gene expression.

The expression of chemokines does not seem to depend strictly on induction by cytokines. In the brains of triple knockout mice, lacking T- and B-cells and functional IFNγ- and IFNα/β-receptors, the expression of CXCL10 and CCL5 is markedly induced after BDV-infection, suggesting that BDV is able to activate the expression of these two chemokines through alternative signaling pathways (Sauder et al., 2000). In brains of the mentioned triple knockout mice, only few scattered CXCL10-expressing astrocytes were found. The presence of functional IFNα/β-receptors

enhanced the number of these CXCL10-positive cells, suggesting that virus-induced IFN might serve to amplify CXCL10-synthesis in BDV-infected brains (Sauder et al., 2000). BDV-infected neurons, extremely abundant and distributed fairly evenly, probably do not contribute to the production of chemokine inducing factors, since CXCL10-positive astrocytes were found only scattered in the brains of the triple knockout animals infected with BDV (Sauder et al., 2000).

In conclusion, we found a striking similarity between the retina and the brain of BDV-infected rats with respect to cytokine and chemokine expression profiles, recruitment of infiltrating immune cells, and activation of resident cells. The early appearance of CD4-positive and CD8-positive T-cells and the expression of T-cell specific cytokines as IFNγ, TNFβ and IL10 differ from the observations in the brains of immunotolerant BDV-infected rats. This suggests identical immunopathological mechanisms to be operative in both the brain and the retina of infected immunocompetent rats.

The retina represents a suitable model region for investigations in the CNS, because of its well defined laminated organization and the exposed position, permitting clinical examination. These retinal advantages together with the data presented here emphasize the BDV-infected retina as a valuable model to study interactions of neural cells and the immune system.

Acknowledgements

This work was supported by the Bundesministerium für Bildung, Forschung und Technologie (BMB+F), interdisciplinary Center for Clinical Research at the University of Leipzig (01KS9504, Project C5).

This study was supported by the Deutsche Forschungsgemeinschaft (Project PA 615/1-1) (J.K. and T.P.).

The authors want to thank Prof. V. Bigl for providing generous access to technological equipment and Margrit Hollborn and Andrea Schwarze for their excellent technical assistance.

References

Asensio, V.C., Campbell, I.L., 1997. Chemokine gene expression in the brains of mice with lymphocytic choriomeningitis. J. Virol. 71, 7832–7840.

Bilzer, T., Planz, O., Lipkin, W.I., Stitz, L., 1995. Presence of CD4+ and CD8+ T cells and expression of MHC class I and MHC class II antigen in horses with Borna disease virus-induced encephalitis. Brain Pathol. 5, 223–230.

Broderick, C., Duncan, L., Taylor, N., Dick, A.D., 2000. IFN-gamma and LPS-mediated IL-10-dependent suppression of retinal microglial activation. Invest. Ophthalmol. Visual Sci. 41, 2613–2622.

Carbone, K.M., Moench, T.R., Lipkin, W.I., 1991. Borna disease virus replicates in astrocytes, Schwann cells and ependymal cells in persistently infected rats: location of viral genomic and messenger RNAs by in situ hybridization. J. Neuropathol. Exp. Neurol. 50, 205–214.

Carbone, K.M., Rubin, S.A., Sierra-Honigmann, A.M., Lederman, H.M., 1993. Characterization of a glial cell line persistently infected with Borna disease virus (BDV): influence of neurotrophic factors on BDV protein and RNA expression. J. Virol. 67, 1453–1460.

Charles, P.C., Chen, X., Horwitz, M.S., Brosnan, C.F., 1999. Differential chemokine induction by the mouse adenovirus type-1 in the central nervous system of susceptible and resistant strains of mice. J. Neurovirology 5, 55–64.

Crane, I.J., Wallace, C.A., McKillop-Smith, S., Forrester, J.V., 2000. Control of chemokine production at the blood–retina barrier. Immunology 101, 426–433.

Cuff, C.A., Berman, J.W., Brosnan, C.F., 2000. Interleukin-1beta-induced expression of monocyte chemotactic protein-1 in the rabbit retina: an in situ and immunohistochemical study. Glia 30, 279–289.

de Kozak, Y., Naud, M.C., Bellot, J., Faure, J.P., Hicks, D., 1994. Differential tumor necrosis factor expression by resident retinal cells from experimental uveitis-susceptible and-resistant rat strains. J. Neuroimmunol. 55, 1–9.

de la Torre, J.C., 1994. Molecular biology of Borna disease virus: prototype of a new group of animal viruses. J. Virol. 68, 7669–7675.

Deschl, U., Stitz, L., Herzog, S., Frese, K., Rott, R., 1990. Determination of immune cells and expression of major histocompatibility complex class II antigen in encephalitic lesions of experimental Borna disease. Acta Neuropathol. (Berl.) 81, 41–50.

Devine, L., Lightman, S.L., Greenwood, J., 1996. Role of LFA-1, ICAM-1, VLA-4 and VCAM-1 in lymphocyte migration across retinal pigment epithelial monolayers in vitro. Immunology 88, 456–462.

Elner, S.G., Strieter, R., Bian, Z.M., Kunkel, S., Mokhtarzaden, L., Johnson, M., Lukacs, N., Elner, V.M., 1998. Interferon-induced protein 10 and interleukin 8. C-X-C chemokines present in proliferative diabetic retinopathy. Arch. Ophthalmol. 12, 1597–1601.

Geiss, V., Frese, K., Morales, J.A., Ojok, L., Herzog, S., 1990. Borna disease virus-induced retinitis in Lewis rats—an immune-mediated retinopathy. Lens Eye Toxic. Res. 7, 741–751.

Glabinski, A.R., Ransohoff, R.M., 1999. Chemokines and chemokine receptors in CNS pathology. J. Neurovirology 5, 3–12.

Gonzalez-Dunia, D., Sauder, C., de la Torre, J.C., 1997. Borna disease virus and the brain. Brain Res. Bull. 44, 647–664.

Gullapalli, V.K., Zhang, J., Pararajasegaram, G., Rao, N.A., 2000. Hematopoietically derived retinal perivascular microglia initiate uveoretinitis in experimental autoimmune uveitis. Graefe Arch. Clin. Exp. Ophthalmol. 238, 319–325.

Hatalski, C.G., Hickey, W.F., Lipkin, W.I., 1998. Evolution of the immune response in the central nervous system following infection with Borna disease virus. J. Neuroimmunol. 90, 137–142.

Herzog, S., Kompter, C., Frese, K., Rott, R., 1984. Replication of Borna disease virus in rats: age-dependent differences in tissue distribution. Med. Microbiol. Immunol. (Berl.) 173 (4), 171–177.

Hesselgesser, J., Horuk, R., 1999. Chemokine and chemokine receptor expression in the central nervous system. J. Neurovirology 5, 13–26.

Holtkamp, G.M., Kijlstra, A., Peek, R., de Vos, A.F., 2001. Retinal pigment epithelium–immune system interactions: cytokine production and cytokine-induced changes. Prog. Retin. Eye Res. 20, 29–48.

Hornig, M., Weissenbock, H., Horscroft, N., Lipkin, W.I., 1999. An infection-based model of neurodevelopmental damage. Proc. Natl. Acad. Sci. U. S. A. 96, 12102–12107.

Kacza, J., Vahlenkamp, T.W., Enbergs, H., Richt, J.A., Germer, A., Kuhrt, H., Reichenbach, A., Muller, H., Herden, C., Stahl, T., Seeger, J., 2000. Neuron–glia interactions in the rat retina infected by Borna disease virus. Arch. Virol. 145, 127–147.

Kacza, J., Mohr, C., Pannicke, T., Kuhrt, H., Dietzel, J., Flüss, M., Richt, J.A., Vahlenkamp, T.W., Stahl, T., Reichenbach, A., Seeger, J., 2001. Changes of the organotypic retinal organization in Borna virus-infected Lewis rats. J. Neurocytol. 30, 801–820.

Krey, H.F., Ludwig, H., Boschek, C.B., 1979a. Multifocal retinopathy in Borna disease virus infected rabbits. Am. J. Ophthalmol. 87, 157–164.

Krey, H., Ludwig, H., Rott, R., 1979b. Spread of infectious virus along the

optic nerve into the retina in Borna disease virus-infected rabbits. Arch. Virol. 61, 283–288.

Kroese, F.G., Wubbena, A.S., Opstelten, D., Deenen, G.J., Schwander, E.H., De Leij, L., Vos, H., Poppema, S., Volberda, J., Nieuwenhuis, P., 1987. B lymphocyte differentiation in the rat: production and characterization of monoclonal antibodies to B lineage-associated antigens. Eur. J. Immunol. 17, 921–928.

Lane, T.E., Asensio, V.C., Yu, N., Paoletti, A.D., Campbell, I.L., Buchmeier, M.J., 1998. Dynamic regulation of alpha- and beta-chemokine expression in the central nervous system during mouse hepatitis virus-induced demyelinating disease. J. Immunol. 160, 970–978.

Mesri, M., Liversidge, J., Forrester, J.V., 1994. ICAM-1/LFA-1 interactions in T-lymphocyte activation and adhesion to cells of the blood-retina barrier in the rat. Immunology 83, 52–57.

Morimoto, K., Hooper, D.C., Bornhorst, A., Corisdeo, S., Bette, M., Fu, Z.F., Schafer, M.K., Koprowski, H., Weihe, E., Dietzschold, B., 1996. Intrinsic responses to Borna disease virus infection of the central nervous system. Proc. Natl. Acad. Sci. U. S. A. 93, 13345–13350.

Munoz-Fernandez, M.A., Fresno, M., 1998. The role of tumor necrosis factor, interleukin 6, interferon-gamma and inducible nitric oxide synthase in the development and pathology of the nervous system. Prog. Neurobiol. 56, 307–340.

Narayan, O., Herzog, S., Frese, K., Scheefers, H., Rott, R., 1983a. Pathogenesis of Borna disease in rats: immune-mediated viral ophthalmoencephalopathy causing blindness and behavioral abnormalities. J. Infect. Dis. 148, 305–315.

Narayan, O., Herzog, S., Frese, K., Scheefers, H., Rott, R., 1983b. Behavioral disease in rats caused by immunopathological responses to persistent Borna virus in the brain. Science 220, 1401–1403.

Noske, K., Bilzer, T., Planz, O., Stitz, L., 1998. Virus-specific CD4+ T cells eliminate Borna disease virus from the brain via induction of cytotoxic CD8+ T cells. J. Virol. 72, 4387–4395.

Pannicke, T., Weick, M., Uckermann, O., Wheeler-Schilling, T., Fries, J.E., Reichel, M.B., Mohr, C., Stahl, T., Fluess, M., Kacza, J., Seeger, J., Richt, J.A., Reichenbach, A., 2001. Electrophysiological alterations and upregulation of ATP receptors in retinal glial Muller cells from rats infected with the Borna disease virus. Glia 35, 213–223.

Planz, O., Bilzer, T., Sobbe, M., Stitz, L., 1993. Lysis of major histocompatibility complex class I-bearing cells in Borna disease virus-induced degenerative encephalopathy. J. Exp. Med. 178, 163–174.

Planz, O., Bilzer, T., Stitz, L., 1995. Immunopathogenic role of T-cell subsets in Borna disease virus-induced progressive encephalitis. J. Virol. 69, 896–903.

Richt, J.A., Stitz, L., Wekerle, H., Rott, R., 1989. Borna disease, a progressive meningoencephalomyelitis as a model for CD4+ T cell-mediated immunopathology in the brain. J. Exp. Med. 170, 1045–1050.

Sauder, C., de la Torre, J.C., 1999. Cytokine expression in the rat central nervous system following perinatal Borna disease virus infection. J. Neuroimmunol. 96, 29–45.

Sauder, C., Hallensleben, W., Pagenstecher, A., Schneckenburger, S., Biro, L., Pertlik, D., Hausmann, J., Suter, M., Staeheli, P., 2000. Chemokine gene expression in astrocytes of Borna disease virus-infected rats and mice in the absence of inflammation. J. Virol. 74, 9267–9280.

Schneemann, A., Schneider, P.A., Lamb, R.A., Lipkin, W.I., 1995. The remarkable coding strategy of Borna disease virus: a new member of the nonsegmented negative strand RNA viruses. Virology 210, 1–8.

Shankar, V., Kao, M., Hamir, A.N., Sheng, H., Koprowski, H., Dietzschold, B., 1992. Kinetics of virus spread and changes in levels of several cytokine mRNAs in the brain after intranasal infection of rats with Borna disease virus. J. Virol. 66, 992–998.

Staeheli, P., Sauder, C., Hausmann, J., Ehrensperger, F., Schwemmle, M., 2000. Epidemiology of Borna disease virus. J. Gen. Virol. 81, 2123–2135 (Pt. 9).

Stitz, L., Krey, H., Ludwig, H., 1981. Borna disease in rhesus monkeys as a models for uveo-cerebral symptoms. J. Med. Virol. 6, 333–340.

Stitz, L., Dietzschold, B., Carbone, K.M., 1995. Immunopathogenesis of Borna disease. Curr. Top. Microbiol. Immunol. 190, 75–92.

Stitz, L., Noske, K., Planz, O., Furrer, E., Lipkin, W.I., Bilzer, T., 1998. A functional role for neutralizing antibodies in Borna disease: influence on virus tropism outside the central nervous system. J. Virol. 72, 8884–8892.

Verma, M.J., Lloyd, A., Rager, H., Strieter, R., Kunkel, S., Taub, D., Wakefield, D., 1997. Chemokines in acute anterior uveitis. Curr. Eye Res. 16, 1202–1208.

Zhao, B., Schwartz, J.P., 1998. Involvement of cytokines in normal CNS development and neurological diseases: recent progress and perspectives. J. Neurosci. Res. 52, 7–16.

Zlotnik, A., Yoshie, O., 2000. Chemokines: a new classification system and their role in immunity. Immunity 12, 121–127.